DOI: https://doi.org/10.62985/j.huit_ojs.vol26.no1E.335

IMPROVING DYNAMIC RESPONSE IN DC MOTOR-GENERATOR SYSTEMS

Luu Hong Quan*, Dang Nguyen Dang Khoa

Faculty of Electrical and Electronics Engineering,

Ho Chi Minh City University of Industry and Trade, Vietnam

*Email: *quanlh@huit.edu.vn*

Received: 3 October 2025; Revised: 17 March 2026; Accepted: 2 April 2026

ABSTRACT

This paper investigates the integration of a proportional-integral-derivative (PID) controller with a Kalman filter to enhance the dynamic response of a direct-current (DC) motor-generator system operating under variable load conditions. The Kalman filter is employed to estimate and smooth the speed signal obtained from the encoder, thereby attenuating measurement noise and providing a more accurate feedback signal to the PID controller. Experimental results demonstrate that the combined Kalman-PID approach significantly improves speed stability, suppresses oscillations, and elevates overall control performance. This methodology shows considerable promise for implementation in modern generator systems that frequently encounter load fluctuations and external disturbances.

Keywords: PID controller, Kalman filter, speed control, state-space model, Arduino-based implementation, noise reduction.

1. INTRODUCTION

In the field of electric drive control, a variety of methods have been developed to enhance dynamic response and maintain system stability under varying load conditions. The PID controller remains a widely utilized approach due to its simple structure and ease of deployment [1], [2]; however, its performance can significantly deteriorate in the presence of noise, nonlinearities, or dynamic delays. To address these limitations, several advanced control strategies have been proposed, including fuzzy control [3], optimal Linear Quadratic Regulator (LQR) control [4], sliding mode control (SMC) [5], and various forms of adaptive control. Fuzzy control enables nonlinear handling without a precise system model but depends heavily on the design of inference rules. LQR provides optimal performance yet requires an accurate state-space model. SMC offers strong disturbance rejection but often introduces chattering effects, whereas adaptive control is suitable for systems with time-varying parameters but entails a more complex control architecture [6], [7].

In addition, advanced techniques such as Model Predictive Control (MPC) have been studied to achieve higher performance in large-scale systems, although their computational demand limits practical implementation on low-cost embedded platforms. Recently, the integration of a Kalman filter with a PID controller has attracted considerable interest due to its ability to mitigate noise measurement and improve feedback quality [8], making it particularly suitable for small-scale motor-drive systems using accessible hardware such as Arduino. These approaches reflect the broader trend in modern control toward solutions that ensure both fast dynamic response and robust performance under load variations [9], [10].

2. THEORETICAL BASIS AND RESEARCH METHODOLOGY

2.1. Theoretical basis

During the research process, analyzing the factors affecting the relationship between machine speed and related technical parameters plays a key role in optimizing operational performance and improving system control capability.

Relationship between DC generator speed and load

The induced EMF in a DC generator is expressed as [11]:

$$E = k \cdot \Phi \cdot N \quad (1)$$

Where:

E is induced EMF (V); k is machine constant; Φ is flux per pole (Wb); N is rotational speed (rpm)

When under load, the output voltage is given as [12]:

$$V = E - I_a \cdot R_a \quad (2)$$

Where:

V is terminal voltage (V); I_a is armature current (A); R_a is armature resistance (Ω)

From (2), when the load increases, I_a increases, leading to a voltage drop.

Relationship between speed and load

For constant terminal voltage [13]:

$$N = \frac{V + I_a \cdot R_a}{k \cdot \Phi} \quad (3)$$

Where:

N is speed (rpm); V is terminal voltage (V); I_a is load current (A); R_a is armature resistance (Ω);

When the load increases, I_a increases, requiring higher speed N to compensate for the voltage drop.

If speed is constant, voltage decreases when load increases.

The rotational speed of a DC motor is directly proportional to the induced electromotive force (EMF). When the mechanical load increases, the armature current also increases, resulting in a reduction of the induced voltage due to internal losses. To compensate for this drop and maintain a stable output voltage, the motor must either increase its rotational speed or adjust the magnetic flux Φ.

In this study, the DC motor operates under variable load conditions on the generator side. Therefore, dynamically regulating the motor speed is critical to stabilizing the generator's output voltage, ensuring rapid transient response and high steady-state accuracy. The PID feedback control strategy is adopted due to its simplicity, robustness, and proven effectiveness in handling nonlinearity and disturbance variations in electromechanical systems.

2.2. State-space model of the DC motor and design of the Kalman filter

2.2.1. DC motor model [14]

The DC motor can be described by the following electrical and mechanical equations:

$$\begin{cases} V(t) = La\frac{di_a(t)}{dt} + R_a i_a(t) + K_e \omega(t) \\ K_t i_a(t) = J\frac{d\omega(t)}{dt} + B\omega(t) \end{cases} \quad (4)$$

Where:

$V(t)$ is the applied armature voltage (V); $i_a(t)$ is the armature current (A); R_a is the armature resistance (Ω); L_a is the armature inductance (H); K_e is the back electromotive force (EMF) constant (V·s/rad); K_t is the torque constant (N·m/A); J is the rotor moment of inertia (kg·m²); B is the viscous friction coefficient (N·m·s/rad); $\omega(t)$ is the angular velocity (rad/s).

2.2.2. State-space representation [15]

Assume that the state vector is defined as:

$$x(t) = \begin{cases} i_a(t) \\ \omega(t) \end{cases}, u(t) = V(t), y(t) = \omega(t) \tag{5}$$

Accordingly, the state-space model of the DC motor can be expressed as follows:

$$\begin{cases} \dot{x}(t) = Ax(t) + Bu(t) \\ y(t) = Cx(t) + Du(t) \end{cases} \tag{6}$$

In which the matrices are given as follows:

$$A = \begin{cases} -\frac{R_a}{L_a} & -\frac{K_e}{L_a} \\ \frac{K_t}{J} & -\frac{B}{J} \end{cases}, B = \begin{cases} \frac{1}{L_a} \\ 0 \end{cases}, C = |0 \quad 1|, D = 0 \tag{7}$$

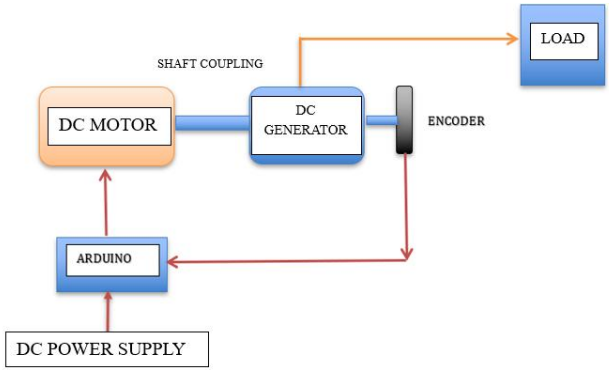

Figure 1. Connection diagram of the DC motor–generator controlled by PID through Arduino

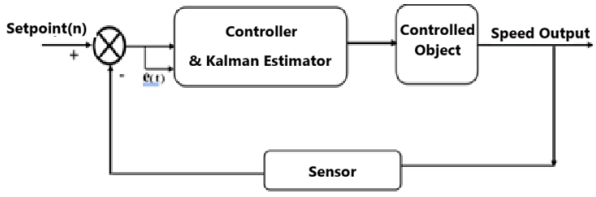

Figure 2. Schematic diagram of the structure applying a PID controller and a Kalman filter

The speed encoder measures the actual rotational speed of the plant and provides this value as a feedback signal to the control system. A Kalman estimator is employed to process the difference between the reference input (setpoint) and the measured speed. This estimator not only assists in generating the control signal but also supports state estimation, effectively distinguishing the true system dynamics (e.g., actual speed) from measurement noise.

In this configuration, the feedback loop is based on speed rather than position, as the encoder specifically measures rotational velocity. The comparator block evaluates the discrepancy between the reference speed and the feedback signal, resulting in the error term $e(t)$, which is used to drive the controller.

The resulting control input $u(t)$from the PID controller is computed based on three components: proportional (P), integral (I), and derivative (D). These components work together to minimize the speed error, improve dynamic performance, and ensure system stability [16], [17].

$$u(t) = K_p.e(t) + K_i.\int e(t)dt + K_d.\frac{de(t)}{dt} \tag{8}$$

Where:

$e(t)$is the error between the desired speed and the actual speed;

$u(t)$is the control signal.

K_p, K_i, and K_d are the proportional, integral, and derivative gains, respectively. Based on these components, the system adjusts the speed by varying the control signal $u(t)$.

During the feedback control process, speed measurement from the encoder introduces several errors, such as inaccurate speed measurement, unstable fluctuations, and oscillations around the setpoint. These issues affect system reliability and reduce equipment lifetime, as prolonged instability can cause wear and tear of joints, bearings, gears, and structural components.

For these reasons, improving the dynamic response under variable load conditions is essential. When the load changes suddenly (increase or decrease), the actual motor speed may oscillate. With more accurate state estimation provided by the Kalman filter, deviations can be identified and corrected more quickly, allowing the system to recover to the desired speed.

The Kalman filter improves system dynamics by reducing settling time and minimizing overshoot or undershoot in the output response. When encoder-based speed measurements are corrupted by noise arising from vibration, power fluctuations, electrical interference, or sensor inaccuracies, the filter processes the raw signal to generate a smooth and reliable estimate. By mitigating noise effects and refining the feedback signal, the Kalman filter reduces the input error to the controller and enhances overall control precision.

In practical applications, the system is subjected to various uncertainties, including fluctuations in supply voltage, changes in motor parameters, mechanical friction, auxiliary load variations, and external disturbances. Despite these nonlinearities and model inaccuracies, the Kalman filter enables accurate state estimation under both moderate and high noise conditions, thereby improving robustness and ensuring stable control performance.

When combined with the PID controller, the speed signal pre-processed by the Kalman filter allows smoother PID operation, reducing oscillations caused by noise or measurement errors, leading to smaller steady-state errors.

Moreover, the Kalman filter helps maintain PID performance by compensating for temporary sensor signal loss or measurement delays, thereby preventing degradation of control accuracy and stability, by predicting the state during uncertain measurement intervals.

2.2.3. Fundamental principle of the Kalman filter [18]

When implementing the model in the discrete-time domain with a sampling period T_s, we have:

$$\begin{cases} x_{k+1} = A_d x_k + B_d u_k + w_k \\ y_k = C x_k + v_k \end{cases} \quad (9)$$

Where:

$w_k \sim \mathcal{N}(0, Q)$denotes the process noise, representing the intrinsic disturbances within the system. $v_k \sim \mathcal{N}(0, R)$ denotes the measurement noise, accounting for errors in the measurement process.

$$A_d = I + AT_s, B_d = BT_s \quad (10)$$

The discrete-time matrices (obtained using first-order approximation) are computed as follows:

The Kalman filter consists of two main stages, formulated as follows:

Prediction stage: Uses data from step $k-1$to calculate the predicted state $\hat{x}_{k|k-1}$and the predicted covariance $P_{k|k-1}$of the system:

State prediction at time k [19]:

$$\hat{x}_{k|k-1} = A\hat{x}_{k-1|k-1} + Bu_k \quad (11)$$

Error covariance prediction [19]:

$$P_{k|k-1} = AP_{k-1|k-1}A^T + Q \quad (12)$$

Where:

$\hat{x}_{k|k-1}$: predicted state; A: system state matrix; B: input control matrix; P: error covariance matrix; Q: process noise covariance

Update stage: The predicted state and covariance are updated using the measurement value.

The Kalman gain $K_k$is updated as follows [19]:

$$K_k = P_{k|k-1}H^T(HP_{k|k-1}H^T + R)^{-1} \quad (13)$$

The state estimate at time step $k$is updated as follows [20]:

$$\hat{x}_{k|k} = \hat{x}_{k|k-1} + K_k(z_k - H\hat{x}_{k|k-1}) \quad (14)$$

The covariance matrix is updated at time step $k$as follows [20]:

$$P_{k|k} = (I - K_k H)P_{k|k-1} \quad (15)$$

Where: K_k is the Kalman gain; Z_k is the measurement input obtained from the encoder; H is the observation matrix; R is the covariance matrix of the measurement noise; Q is the covariance matrix of the process noise.

2.3. Design and implementation of the motor–generator model

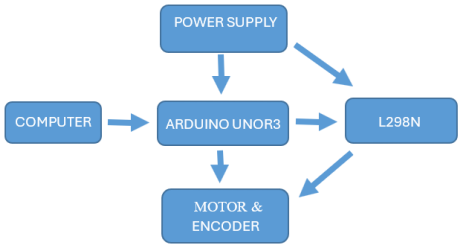

Figure 3. Control block diagram

Power block is 12V DC power supply for the L298N circuit.

The JGB37-520 is a 12-VDC geared motor equipped with an encoder, providing an output speed of approximately 333 rpm.

Table 1. Specifications of the JGB37-520 motor

Parameter	Symbol	Value (SI Units)
Armature resistance	Ra	10 Ω
Armature inductance	La	0.45 mH = 4.5×10⁻⁴ H
Back electromotive force (EMF) constant	Ke	0.34 V·s/rad
Torque constant	Kt	0.034 N·m/A
Moment of inertia	J	7.0×10⁻⁶ kg·m²
Viscous friction coefficient	B	1.6×10⁻⁴ N·m·s/rad
Sampling period	T_s	1 ms = 0.001 s

The control circuit block is the L298N driver providing power to the DC motor with Encoder through the two output pins Out1 and Out2. At the same time, it receives control signals from Arduino PWM pins 9, 8, and 7, which are connected to Ena, In1, and In2.

Arduino Uno R3 is programmed via laptop to control the circuit.

Power stage block is the part where the DC motor with encoder rotates and sends pulse signals back to the Arduino.

Figure 4. Control boards and encoder module

By manually tuning the controller parameters, the selected PID gains are $K_p = 2.5$, $K_i = 2$, and $K_d = 0.1$

3. RESULTS AND DISCUSSION

The motor-generator model was implemented by the authors as an experimental prototype.

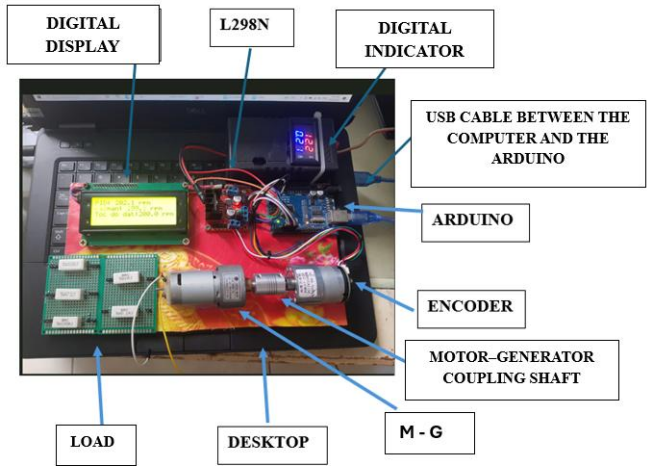

Figure 5. Experimental model of the DC motor–generator system

The experimental process with different load conditions at a set speed of 200 rpm yielded the waveforms shown in Figures 6, 7, and 8, along with the corresponding comparison tables.

3.1. No loading

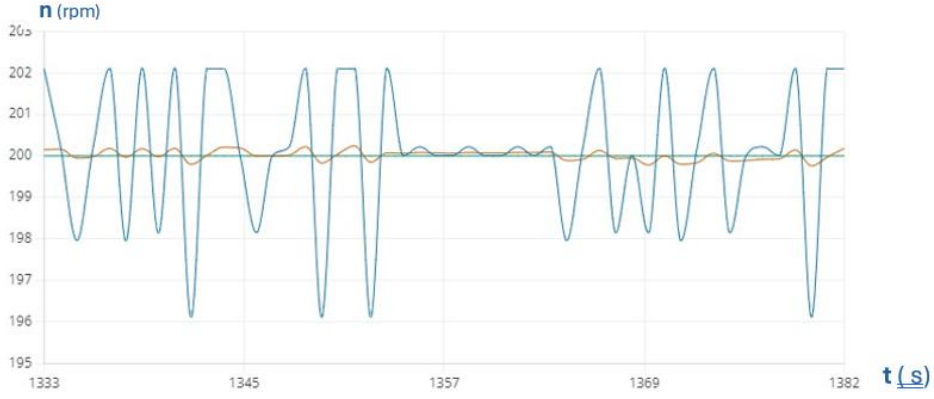

Figure 6. Waveform under no-load condition

Table 2. Comparison under no-load condition

Attributes	Without Kalman (Blue)	With Kalman (Brown)
Min	196	199
Max	202	201
Amplitude (Max - Min)	6	2

Table 3. Comparison of performance indicators no-load

Indicator	Without Kalman (Blue)	With Kalman (Orange)	Remarks
Settling time	≈ 1.5–2 s	≈ 1.0 s	Kalman filter helps the system reach stability faster.
Overshoot	1.5–2 rpm (~1%)	< 0.3 rpm (~0.15%)	Significantly reduces overshoot oscillations.
Steady-state error	±0.3 rpm	±0.05 rpm	Kalman improves steady-state accuracy.
ISE ($\int e^2 dt$)	High (due to large noise)	Very low	Kalman filtering smooths the signal and reduces squared error.
RMS noise	≈ 0.6–0.8 rpm	≈ 0.1–0.2 rpm	Kalman significantly reduces measurement noise.

No loading conclusion

The Kalman filter effectively reduces random noise, enhances system stability, minimizes steady-state error and overshoot — resulting in a smoother and more accurate rotational speed response.

3.2. Light loading

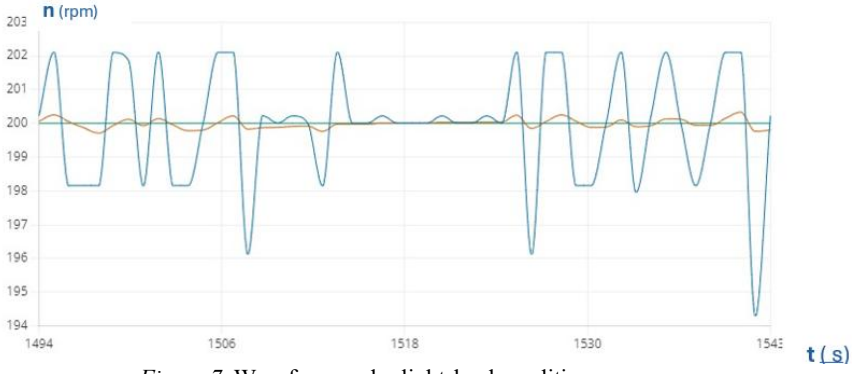

Figure 7. Waveform under light-load condition

Table 4. Comparison under light-load condition

Attributes	Without Kalman (Blue)	With Kalman (Brown)
Min	195	199
Max	202	201
Amplitude (Max – Min)	7	2

Table 5. Comparison of performance indicators light load

Indicator	Without Kalman (Blue)	With Kalman (Orange)	Remarks
Settling time	≈ 1.5–2 s	≈ 1.0 s	Kalman filter helps the system reach stability faster.
Overshoot	1.5–2 rpm (~1%)	< 0.3 rpm (~0.15%)	Significantly reduces overshoot oscillations.
Steady-state error	±0.3 rpm	±0.05 rpm	Kalman improves steady-state accuracy.
ISE ($\int e^2 dt$)	High (due to large noise)	Very low	Kalman filtering smooths the signal and reduces squared error.
RMS noise	≈ 0.6–0.8 rpm	≈ 0.1–0.2 rpm	Kalman significantly reduces measurement noise.

Light loading conclusion

The Kalman filter effectively reduces random noise, enhances system stability, minimizes steady-state error and overshoot — resulting in a smoother and more accurate rotational speed response.

3.3. Heavy loading

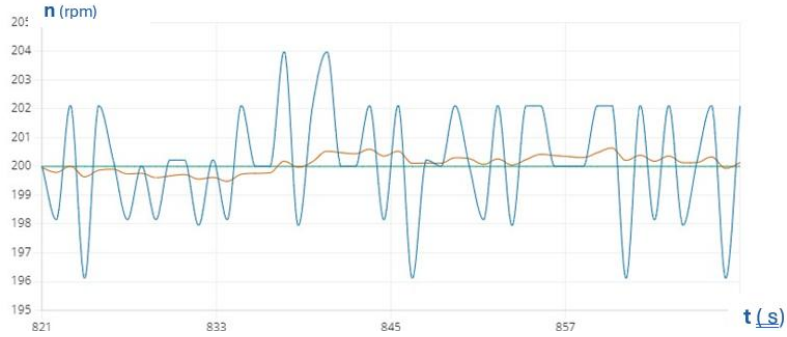

Figure 8. Waveform under heavy-load condition

Table 6. Comparison under heavy-load condition

Attributes	Without Kalman (Blue)	With Kalman (Brown)
Min	196	199
Max	204	201
Amplitude (max – min)	8	2

Table 7. Comparison of performance indicators heavy load

Indicator	Without Kalman (Blue)	With Kalman (Orange)	Remarks
Settling time	≈ 2.0 s	≈ 1.0 s	Kalman filter helps the signal stabilize faster.
Overshoot	≈ +3 rpm (≈ 1.5%)	≈ +0.5 rpm (≈ 0.25%)	Significantly reduces peak oscillations.
Steady-state error	±0.4 rpm	±0.05 rpm	Kalman improves steady-state accuracy.
ISE ($\int e^2 dt$)	High (due to large noise amplitude)	Very low	Considerably reduces squared error.
RMS noise	≈ 0.7–0.9 rpm	≈ 0.1–0.2 rpm	Kalman reduces measurement noise by about 80–90%.

Heavy loading conclusion

The Kalman filter enables faster stabilization of the speed signal, significantly reduces noise and overshoot, and enhances the overall accuracy and smoothness of the system.

Remarks are based on the data presented in the previous tables, and considering all three operating cases, the following comparison of oscillation amplitudes is obtained:

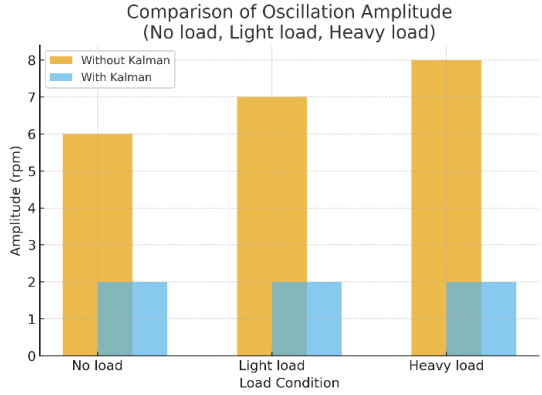

Figure 9. Oscillation amplitude under different load conditions

The stability improvement achieved by incorporating the Kalman filter, compared to the system without filtering, is quantified as 66.7% under no-load conditions, 71.4% under light-load conditions, and 75.0% under heavy-load conditions. These results indicate that the Kalman filter becomes increasingly effective as the load increases, with stability enhancements reaching up to 75% relative to the unfiltered measurements.

4. CONCLUSION

The research and experimental results have demonstrated that combining the PID controller with the Kalman filter brings significant improvements in enhancing the dynamic response of the DC motor–generator system. The Kalman filter smooths the speed signal, greatly reduces noise and oscillations, and maintains the motor speed closer to the setpoint under all load conditions.

Specifically, the oscillation amplitude was reduced from 6–8 rpm (without Kalman) down to only 2 rpm (with Kalman), corresponding to a stability improvement of 66.7% at no-load, 71.4% at light load, and 75.0% at heavy load**.** This result demonstrates that the influence of the Kalman filter becomes more pronounced as the load increases, leading to a significant improvement in both the dynamic response and long-term stability of the system.

In conclusion, the study confirms the crucial role of the Kalman filter in improving motor speed control quality, opening up effective applications in modern DC generator control systems where load conditions and disturbances vary continuously and unpredictably.

Across all operating conditions — no load, light load, and heavy load — the Kalman filter demonstrates a consistent and significant improvement in system performance. It effectively suppresses measurement noise, accelerates the settling response, and minimizes overshoot and steady-state error. The filtered speed signal becomes smoother and more stable, ensuring accurate estimation even under varying load disturbances.

These results confirm that the Kalman filter enhances both the dynamic and steady-state characteristics of the DC motor speed control system. Its robustness against sensor noise and load fluctuations makes it a reliable and efficient solution for real-time motor control applications.

REFERENCES

[1] A. M. Almawla, M. J. Hussein, and A. T. Abdullah, “A Comparative Study of DC Motor Speed Control Techniques Using Fuzzy, SMC and PID,” *J. Eur. Systèmes Autom.*, vol. 57, no. 2, pp. 397–406, Apr. 2024, doi: https://doi.org/10.18280/jesa.570209.

[2] S. Balamurugan and A. Umarani, “Study of Discrete PID Controller for DC Motor Speed Control Using MATLAB,” in *2020 International Conference on Computing and Information Technology (ICCIT-1441)*, Tabuk, Saudi Arabia: IEEE, Sep. 2020, pp. 1–6. doi: https://doi.org/10.1109/ICCIT-144147971.2020.9213780.

[3] M. Nassim and A. Abdelkader, “Speed Control of DC Motor Using Fuzzy PID Controller,” 2021, *arXiv*. doi: https://doi.org/10.48550/ARXIV.2108.05450.

[4] M. B. Aremu, M. Abdel-Nasser, N. M. Alyazidi, and A. S. El-Ferik, “Disturbance Observer-Based Bio-Inspired LQR Optimization for DC Motor Speed Control,” *IEEE Access*, vol. 12, pp. 152418–152429, 2024, doi: https://doi.org/10.1109/ACCESS.2024.3478362.

[5] Freitas, J.B.S., Marquezan, L., de Oliveira Evald, P.J.D. et al. A fuzzy-based Predictive PID for DC motor speed control. Int. J. Dynam. Control 12, 2511–2521 (2024). doi: https://doi.org/10.1007/s40435-023-01368-2

[6] S. G. Malla *et al.*, “Whale Optimization Algorithm for PV Based Water Pumping System Driven by BLDC Motor Using Sliding Mode Controller,” *IEEE J. Emerg. Sel. Top. Power Electron.*, vol. 10, no. 4, pp. 4832–4844, Aug. 2022, doi: https://doi.org/10.1109/JESTPE.2022.3150008.

[7] M. H. Setiawan, A. Ma’arif, C. Rekik, A. J. Abougarair, and A. M. Mekonnen, “Enhancing Speed Estimation in DC Motors using the Kalman Filter Method: A Comprehensive Analysis,” *J. Ilm.*

Tek. Elektro Komput. Dan Inform., vol. 10, no. 1, p. 30, Feb. 2024, doi: https://doi.org/10.26555/jiteki.v10i1.26591.

[8] S. Roy and G. L. Raja, "Hybrid Kalman-Sliding Mode Control For Accurate Speed Tracking Of DC Motors," *Procedia Comput. Sci.*, vol. 258, pp. 3231–3240, 2025, doi: https://doi.org/10.1016/j.procs.2025.04.581.

[9] S. Yuliawan, O. Wahyunggoro, and N. Setiawan, "Kalman Filter to Improve Performance of PID Control Systems on DC Motors," *IJITEE Int. J. Inf. Technol. Electr. Eng.*, vol. 5, no. 3, p. 96, Sep. 2021, doi: https://doi.org/10.22146/ijitee.64511.

[10] H. H. Vo, D. V. P. Tran, T. Q. Thieu, T. A. Le, C. S. T. Dong, and P. Brandstetter, "Sliding Mode PWM-Direct Torque Controlled Induction Motor Drive with Kalman Filtration of Estimated Load," *J. Adv. Eng. Comput.*, vol. 5, no. 4, p. 265, Dec. 2021, doi: https://doi.org/10.55579/jaec.202154.342.

[11] S. Mochrie and C. De Grandi, "Faraday's Law and Electromagnetic Induction," in *Introductory Physics for the Life Sciences*, in Undergraduate Texts in Physics., Cham: Springer International Publishing, 2023, pp. 793–829.doi: https://doi.org/10.1007/978-3-031-05808-0_18.

[12] Mehta*, V. K., & Mehta, R. (2002). Principles of electrical machines. S. Chand Publishing*.

[13] Electrical Engineering Dept, University of Nigeria, Nsukka Enugu State Nigeria. *et al.*, "Dynamics of Speed Control of Dc Motor using Combine Armature and Field Control with Pi Controller," *Int. J. Eng. Adv. Technol.*, vol. 9, no. 3, pp. 3585–3591, Feb. 2020, doi: https://doi.org/10.35940/ijeat.C6043.029320.

[14] M. Kuczmann, "Review of DC Motor Modeling and Linear Control: Theory with Laboratory Tests," *Electronics*, vol. 13, no. 11, p. 2225, Jun. 2024, doi: https://doi.org/10.3390/electronics13112225.

[15] Qolil Ariyansyah and A. Ma'arif, "DC Motor Speed Control with Proportional Integral Derivative (PID) Control on the Prototype of a Mini-Submarine," *J. Fuzzy Syst. Control*, vol. 1, no. 1, pp. 18–24, Mar. 2023, doi: https://doi.org/10.59247/jfsc.v1i1.26.

[16] C. Urrea and R. Agramonte, "Kalman Filter: Historical Overview and Review of Its Use in Robotics 60 Years after Its Creation," *J. Sens.*, vol. 2021, no. 1, p. 9674015, Jan. 2021, doi: https://doi.org/10.1155/2021/9674015.

[17] L. Torres, J. Jiménez-Cabas, O. González, L. Molina, and F.-R. López-Estrada, "Kalman Filters for Leak Diagnosis in Pipelines: Brief History and Future Research," *J. Mar. Sci. Eng.*, vol. 8, no. 3, p. 173, Mar. 2020, doi: https://doi.org/10.3390/jmse8030173.

[18] B. Wang, Z. Sun, X. Jiang, J. Zeng, and R. Liu, "Kalman Filter and Its Application in Data Assimilation," *Atmosphere*, vol. 14, no. 8, p. 1319, Aug. 2023, doi: https://doi.org/10.3390/atmos14081319.

[19] L. Ding and C. Wen, "High-Order Extended Kalman Filter for State Estimation of Nonlinear Systems," *Symmetry*, vol. 16, no. 5, p. 617, May 2024, doi: https://doi.org/10.3390/sym16050617.

[20] C. Sheng *et al.*, "A Comparative Study of the Kalman Filter and the LSTM Network for the Remaining Useful Life Prediction of SOFC," *Energies*, vol. 16, no. 9, p. 3628, Apr. 2023, doi: https://doi.org/10.3390/en16093628.